Published online 19 September 2016

Nucleic Acids Research, 2017, Vol. 45, No. 3 ***1455–1468***
doi: 10.1093/nar/gkw823

Competitive regulation of alternative splicing and alternative polyadenylation by hnRNP H and CstF64 determines acetylcholinesterase isoforms

Mohammad Nazim, Akio Masuda†, Mohammad Alinoor Rahman†, Farhana Nasrin, Jun-ichi Takeda, Kenji Ohe, Bisei Ohkawara, Mikako Ito and Kinji Ohno*

Division of Neurogenetics, Center for Neurological Diseases and Cancer, Nagoya University Graduate School of Medicine, Nagoya, Aichi, Japan

Received May 06, 2016; Revised August 11, 2016; Accepted September 07, 2016

ABSTRACT

Acetylcholinesterase (AChE), encoded by the *ACHE* gene, hydrolyzes the neurotransmitter acetylcholine to terminate synaptic transmission. Alternative splicing close to the 3′ end generates three distinct isoforms of $AChE_T$, $AChE_H$ and $AChE_R$. We found that hnRNP H binds to two specific G-runs in exon 5a of human *ACHE* and activates the distal alternative 3′ splice site (ss) between exons 5a and 5b to generate $AChE_T$. Specific effect of hnRNP H was corroborated by siRNA-mediated knockdown and artificial tethering of hnRNP H. Furthermore, hnRNP H competes for binding of CstF64 to the overlapping binding sites in exon 5a, and suppresses the selection of a cryptic polyadenylation site (PAS), which additionally ensures transcription of the distal 3′ ss required for the generation of $AChE_T$. Expression levels of hnRNP H were positively correlated with the proportions of the $AChE_T$ isoform in three different cell lines. HnRNP H thus critically generates $AChE_T$ by enhancing the distal 3′ ss and by suppressing the cryptic PAS. Global analysis of CLIP-seq and RNA-seq also revealed that hnRNP H competitively regulates alternative 3′ ss and alternative PAS in other genes. We propose that hnRNP H is an essential factor that competitively regulates alternative splicing and alternative polyadenylation.

INTRODUCTION

RNA processing, including alternative splicing (AS) and alternative polyadenylation (APA) of pre-mRNA, is a highly specialized mechanism that enables enhanced transcriptome and proteome diversity. AS causes skipping/inclusion of exons or retention of introns through differential selection of splice sites (ss's) in pre-mRNA, and APA results in distinct 3′ ends through regulated processing of the 3′ end including transcription termination, cleavage and polyadenylation (1,2). More than ∼90% of transcripts undergo alternative RNA processing (3), which are estimated to generate ∼100 000 different proteins from ∼20 000 human genes (4,5). Specific *cis*-elements on pre-mRNA and the cognate *trans*-acting factors facilitate coordinated regulation of alternative RNA processing in tissue-specific and developmental stage-specific manners (1,2).

Acetylcholinesterase (AChE) is a serine-specific hydrolase that plays a pivotal role at the central and peripheral cholinergic synapses. AChE hydrolyses and clears acetylcholine (ACh) in the synaptic cleft, and thereby terminates neurotransmission (6). The expression of AChE, however, is not restricted to the cholinergic tissues (7–9). Furthermore, AChE isoforms show complex expression patterns dependent on tissue and cell-type specificity, differentiation state, physiological condition and response to external stimuli; which may provide a link to some previously reported non-classical functions of AChE such as neuritogenesis, synaptogenesis, amyloid fiber assembly, hematopoiesis and thrombopoiesis (6). In vertebrates, the 3′ end of *ACHE* pre-mRNA is alternatively spliced to generate three different isoforms that bear an identical catalytic domain but a distinct C-terminal end (10) (Figure 1): (i) $AChE_T$ - a 'tailed' subunit expressed predominantly in the muscle and brain that can form a tetrameric structure, which anchors to proline-rich membrane anchor PRiMA or trimeric collagen Q tail (11), (ii) $AChE_H$ – a 'hydrophobic' subunit expressed predominantly in hematopoietic cells that dimerizes itself and anchors to the cell membrane using glycophosphatidylinositol (9), and (iii) $AChE_R$ – an unspliced and rare 'readthrough' subunit, which remains as a soluble monomer and is upregulated under acute psychological stress in the mouse brain (12).

*To whom correspondence should be addressed. Tel: +81 52 744 2446; Fax: +81 52 744 2449; Email: ohnok@med.nagoya-u.ac.jp
†These authors contributed equally to the paper.

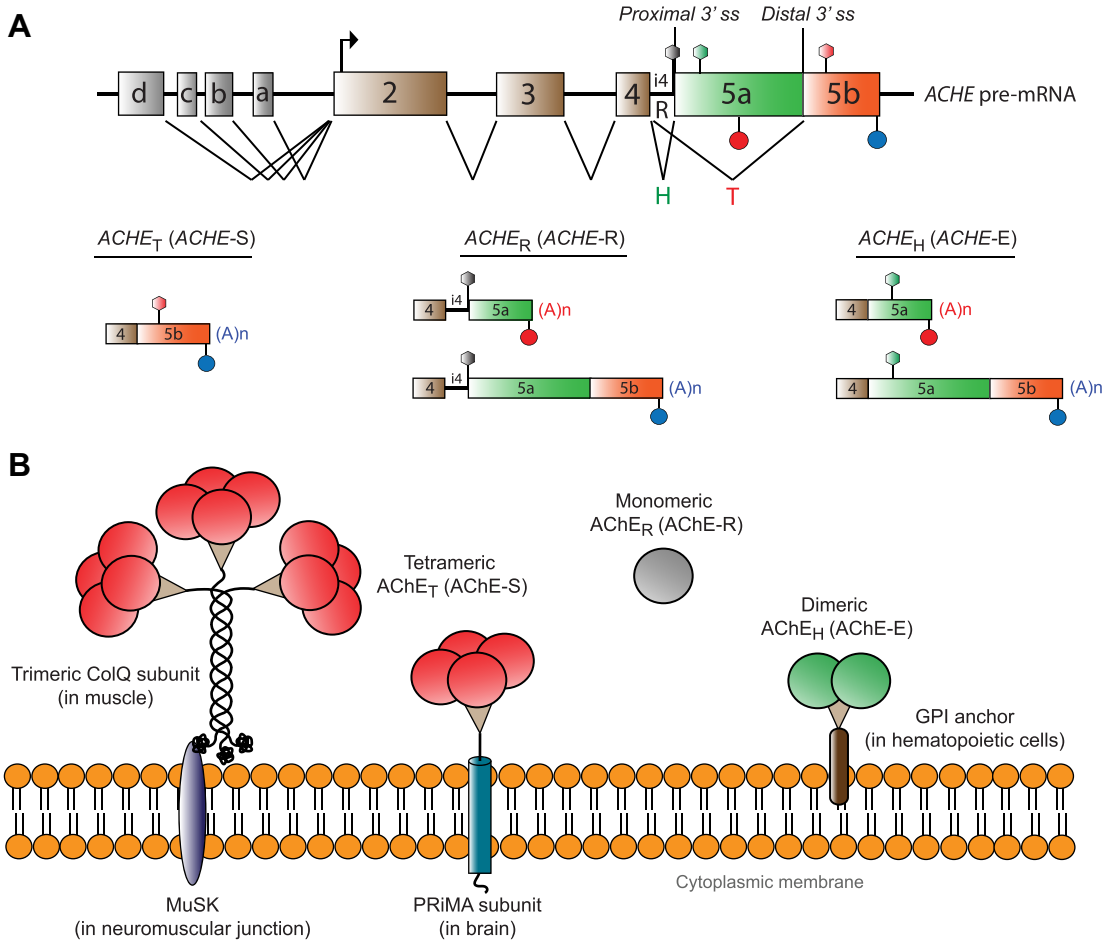

Figure 1. Schematic of alternative splicing of AChE isoforms and their membrane localizations. (**A**) Schematic of genomic structure of human *ACHE* gene locus. Exons and introns are shown in boxes and solid lines, respectively. Gray boxes indicate alternative 5′ exons in the untranslated region (UTR); brown boxes indicate constitutive exons; and green and red boxes are the alternatively spliced terminal exons. Constitutive and alternative splicings are shown by lines connecting exons. Positions of stop codons of AChE$_R$ (gray hexagon), AChE$_H$ (green hexagon) and AChE$_T$ (red hexagon) are indicated above the gene structure. The cryptic (pA-1) and canonical (pA-2) PASs are indicated by red and blue closed circles, respectively, below the gene structure. *ACHE*$_T$, *ACHE*$_H$ and *ACHE*$_R$ transcripts are schematically shown with their aliases. (**B**) Protein structure of AChE isoforms and their localizations in the cellular membrane. AChE$_T$ isoform (red circles) forms a tetrameric structure that anchors to the PRiMA subunit (in brain) or trimeric ColQ subunit (in muscle). ColQ binds to MuSK and perlecan (not shown) at the neuromuscular junction. AChE$_H$ isoform (green circles) forms a dimer that anchors to hematopoietic cell membrane through the GPI anchor. AChE$_R$ isoform (gray circle) is rarely expressed and is a soluble monomer. PRiMA, proline-rich membrane anchor; ColQ, collagen Q; MuSK, muscle-specific receptor tyrosine kinase; and GPI, glycophosphatidylinositol.

ACHE has 5 exons, including 3 invariant exons (exons 2, 3 and 4) that encode the core catalytic domain, and variable 5′ and 3′ regions (12) (Figure 1A). Exon 5 has two alternative 3′ ss's: one at the boundary of intron 4 and exon 5a (proximal 3′ ss) and the other at the boundary of exon 5a and exon 5b (distal 3′ ss). Splicing from exon 4 to exon 5a (selection of the proximal 3′ ss) makes the AChE$_H$ isoform, whereas splicing from exon 4 to exon 5b (selection of the distal 3′ ss) makes the AChE$_T$ isoform. The readthrough AChE$_R$ isoform is generated when the transcript is unspliced after exon 4. In addition to alternative splicing, a tissue-specific alternative polyadenylation site (PAS) is reported ∼1.2 kb downstream to the canonical PAS in the muscle and brain in mouse, as well as in murine erythroleukemia cells (13), which, however, is annotated only in the AceView database in mouse and the H-Inv database in human. Another alternative PAS in exon 5a, which will be experimentally addressed in this communication, is also registered in some annotation databases in human (pA-1 in Supplementary Figure S1), but not in mouse.

To date, several reports have shed light on the regulation of isoform-specific expression of AChE. Guerra *et al.* previously identified the branch point and the polypyrimidine tract, as well as four splicing regulatory *cis*-elements comprised of 5 to 9 nucleotides, in exon 5a in the rat *Ache* gene (Figure 2A, B and Supplementary Figure S2A), although an RNA binding-protein for each *cis*-element was not determined (14). Ubiquitously expressed splicing factors, SRSF1 (SF2/ASF) and SRSF2 (SC-35), were reported to up- and down-regulate the relative expression ratio of human AChE$_T$ to AChE$_R$ transcripts, respectively (15). Splicing *cis*-elements for SRSF1 and SRSF2 were predicted but were not identified. In addition, HuD and HuR stabilize *Ache* mRNA by binding to an AU-rich element in the 3′ UTR in rat and mouse (Supplementary Figure S2A) (16,17). As intron 4 and exon 5a of *ACHE* are poorly con-

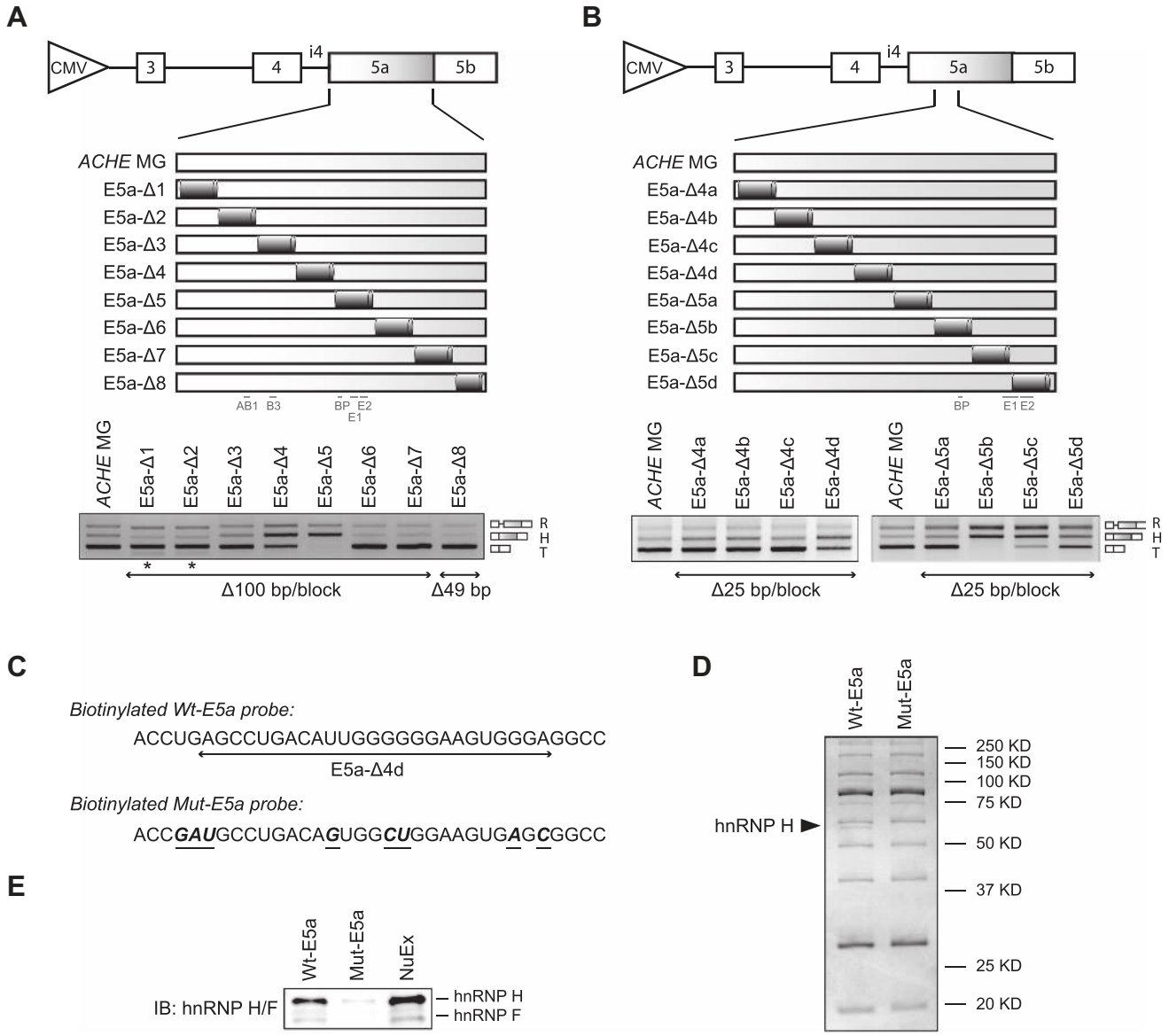

Figure 2. Identification of spicing regulatory *cis*-elements and *trans*-acting factors. (**A** and **B**) Structure of the human *ACHE* minigene (MG) construct spanning exons 3 to 5b, which is driven by a CMV promoter. Schematic of scanning deletion mutagenesis of (**A**) 100-bp and 49-bp blocks of the entire exon 5a and (**B**) 25-bp blocks of E5a-Δ4 and E5a-Δ5. RT-PCR of the wild-type and deletion constructs transfected in SH-SY5Y cells are shown. *ACHE* isoforms are schematically shown on the right side of the gel images. Asterisks indicate that the reverse primer for detecting $AChE_R$ and $AChE_H$ are different from the others, because the primer-binding site is deleted in these constructs. Previously identified regulatory *cis*-elements (AB1, B3, E1, E2 and the branch point (BP)) (14) in rat *Ache* are aligned to human *ACHE*, and are indicated below the schemes. Note that BP is more conserved than the other 4 elements (see Supplementary Figure S2A). (**C**) Sequence of biotinylated wild-type (Wt) and mutant (Mut) E5a probes covering the E5a-Δ4d region. Mutations are shown in bold italic characters with underlines. (**D**) Coomassie blue staining of the RNA affinity-purified proteins of SH-SY5Y nuclear extract using the indicated biotinylated RNA probes. Protein size markers are indicated. Mass spectrometry analysis revealed that a distinct protein band of ~55 kDa (arrowhead) is hnRNP H. (**E**) Immunoblotting of the RNA affinity-purified proteins in (**D**) with an antibody recognizing both hnRNP H and F.

served between human and rodents (Supplementary Figure S2A), we dissected splicing mechanisms of human *ACHE*.

Heterogeneous nuclear ribonucleoproteins (hnRNPs) are ubiquitously expressed RNA-binding proteins that make a complex with heterogeneous nuclear RNA, and play crucial roles in many aspects of RNA processing. HnRNP H (H1, H2 and H3) and hnRNP F belong to a closely related subfamily of hnRNPs (Supplementary Figure S3). HnRNP H2 and hnRNP F are 96% and 68% identical to hnRNP H1, respectively, at the amino acid level (18). HnRNP H3 is the most divergent family member and is smaller than the others with 48% identity to hnRNP H1. HnRNP H3 lacks the first and critical RNA recognition motif (RRM1) and is less likely to have any major effect on splicing regulation (18). As hnRNP H1 and H2 could not be differentiated at the protein level, we collectively indicated hnRNP H1 and H2 as hnRNP H in this communication, like previous reports on hnRNP H by other groups (18,19).

HnRNP H/F preferentially bind to poly(G)-rich sequences (G-runs) in the target exon and/or adjacent introns, and regulate alternative splicing of numerous genes (18,20–27). In addition, hnRNP H/F have been proposed to affect the efficiency of 3′ end-processing. HnRNP H/F interact with cleavage stimulation factor (CstF) 64 and regulate 3′ end-processing of several PASs (28–31). CstF64 is a component of an essential 3′ end-processing factor, CstF, and specifically recognizes the GU/U-rich elements downstream to the cleavage site (2). Additionally, RNA-seq and CLIP-seq analyses revealed that increased binding of hnRNP H upstream of APA sites correlated with the selection of these sites (32). Although these studies documented individual regulations of AS and APA by hnRNP H/F, the relationship between these two mechanisms remain scarcely understood.

In this communication, we dissected the molecular mechanism of alternative 3′ ss selection of human *ACHE* gene. We found that hnRNP H binds to two specific G-runs in exon 5a, and activates the distal 3′ ss to produce $AChE_T$ transcript. We also found that lack of hnRNP H enables binding of CstF64 to GU-rich elements in exon 5a, and activates a cryptic PAS in exon 5a to produce $AChE_H$ and $AChE_R$ transcripts. Interestingly, hnRNP H and CstF64 compete for binding to the overlapping sites in exon 5a. Global analysis of CLIP-seq and RNA-seq data revealed that suppression of alternative PASs by hnRNP H correlates with activation of distal 3′ ss's, as observed in the *ACHE* gene. Our findings thus unveiled an intricate interplay between AS and APA mediated by hnRNP H and CstF64 in the human *ACHE* gene.

MATERIALS AND METHODS

RT-PCR

Total RNA was isolated at 48 h after transfection using the Trizol reagent (Thermo Fisher Scientific) followed by treatment with DNase I (Qiagen). cDNAs were synthesized with an oligo-dT primer (Thermo Fisher Scientific) and ReverTra Ace reverse transcriptase (Toyobo). PCR was performed with GoTaq polymerase (Promega) using primers shown in Supplementary Table 1.

siRNA-mediated knocking down

The HP Validated siRNA (SI02654799, Qiagen) (25) was used to downregulate hnRNP H1 and H2. We also synthesized siRNA against human hnRNP F with the sequence of 5′-GCGACCGAGAACGACAUUU-3′ (Sigma Genosys). To knockdown hnRNP H1, H2 and F together, we synthesized siRNA against a shared segment of human hnRNP H1, H2 and F: 5′-GGAAGAAAUUGUUCAGUUC-3′ (23). To knockdown hnRNP A1 and hnRNP A2/B1, we synthesized siRNAs with the sequence of 5′-CAGCTGAGGAAGCTCTTCA-3′ and 5′-GGAGAGTAGTTGAGCCAAA-3′, respectively. The control siRNA was AllStar Negative Control siRNA (1027281, Qiagen).

RNA affinity purification assay

Biotin-labeled RNA probes were synthesized with the T7 RiboMAX large-scale RNA production system (Promega) using PCR-amplified DNA templates. Briefly, for a 20 μl reaction, we used 7.5 mM UTP, 7.5 mM ATP, 7.5 mM GTP, 4.5 mM CTP and 3.0 mM biotin-14-CTP (Thermo Fisher Scientific) to transcribe 2 μg DNA template by T7 RNA polymerase. The detailed affinity purification method is described in Supplementary Methods (Supplementary Information).

Mass spectrometry

We excised a specific band from the Coomassie blue-stained polyacrylamide gel and performed in-gel digestion by Trypsin Gold (Promega) following the manufacturer's instructions. Nanoelectrospray tandem mass analysis was carried out as previously described (24).

Tethered function assay of hnRNP H and F

Artificial tethering of hnRNP H and F were performed by co-transfection of a reporter minigene carrying a PP7-hairpin loop and an effector construct carrying either hnRNP H or hnRNP F fused to the bacteriophage PP7 coat protein, as previously described (33). We introduced the PP7 hairpin sequence (5′-GGCACAGAAGATATGGCTTCGTGCC-3′) in the minigene by replacing the native *cis*-element sequence in exon 5a (5′-GGGGGGAAGTGGG-3′), using the QuikChange Site-Directed Mutagenesis kit (Agilent).

3′ RACE

We isolated polyA-enriched mRNA using GenElute mRNA Miniprep Kit (Sigma-Aldrich) and performed 3′ RACE as described elsewhere (34). cDNA was synthesized using oligo dT18-XbaKpnBam primer. The 3′ ends were determined by 3′ RACE using nested forward primers and a shared XbaKpnBam reverse primer (Supplementary Table 1) (34).

Depletion of hnRNP H/F and CstF64 from nuclear extract

Antibody-mediated depletion of hnRNP H/F and CstF64 from HeLa nuclear extract (CilBiotech) was carried out using the Protein G HP spin trap (GE Healthcare) following manufacturer's instructions. Depletion of hnRNP H/F and CstF64 was performed with anti-hnRNP F/H (sc-32310, Santa Cruz Biotechnology) and anti-CstF64 (C-20, Santa Cruz Biotechnology) antibodies, respectively.

Bioinformatic analysis

The RNA-seq FASTQ files of HEK293T cells treated with control siRNA or *HNRNPH* siRNA (GSE16642) (32), as well as the CLIP-seq FASTQ files of hnRNP H in HEK 293T cells (GSE23694) (32), were obtained from the NCBI GEO database. The RNA-seq and the CLIP-seq FASTQ files were mapped to the reference human genome (GRCh37/hg19) using TopHat version 2.0.12 (35)

and BWA version 0.7.12 (36) with default parameters, respectively. The RNA-seq BAM files were assembled into transcripts by Cufflinks version 2.2.1 (37) with default parameters. Expression levels of the transcripts were calculated using the Cuffdiff (Cufflinks version 2.2.1) with default parameters. Percent-spliced-in (PSI) of alternative 3′ ss's (A3SS) were calculated using MISO (version 0.5.2) (32) with default parameters. The ΔPSI of control siRNA and *HNRNPH* siRNA were filtered with parameters '–num_inc 1–num-exc 1–delta-psi 0.2–bayes-factor 10'. To remove PCR duplicates of the CLIP-seq BAM files, SAMtools version 0.1.19 was used (38). SAMtools was also used to convert a SAM file into a BAM file, to sort a BAM file, and to make a BAM index file. To calculate density of CLIP-tags, a BedGraph file converted from a BAM file by BEDTools (version 1.1.2) (39) was used.

Other materials and methods

Supplementary material includes additional information on (i) Cell culture, (ii) Construction of *ACHE* minigene for splicing analysis, (iii) Plasmid and siRNA transfection, (iv) Construction of cDNA, (v) RNA affinity purification assay, (vi) Tethered function assay of hnRNP H and F, (vii) Preparation of total cell lysates for immunoblotting, (viii) Preparation of nuclear extracts for immunoblotting and RNA affinity purification, (ix) Cell survival assay, (x) Neuronal differentiation of SH-SY5Y cells, (xi) Antibodies for immunoblotting and (xii) Statistical analysis.

RESULTS

Identification of splicing regulatory *cis*-elements by minigene analysis

In order to dissect *cis*-elements governing isoform-specific alternative splicing of *ACHE*, we first constructed human *ACHE* minigene by cloning exon 3 to exon 5b of *ACHE* in pcDNA 3.1(+) vector (Figure 2A and B). We transfected the *ACHE* minigene into the human neuroblastoma cell line, SH-SY5Y, where dominant expression of $AChE_T$ is observed as in the brain and skeletal muscle (Supplementary Figures S4A and S4B). We found that the splicing pattern of the minigene was similar to that of endogenous *ACHE* in SH-SY5Y cells (Supplementary Figure S4B). We then searched for blocks carrying splicing regulatory *cis*-elements in the alternatively spliced exon 5a. To this end, we sequentially deleted seven 100-bp blocks and one 49-bp block in exon 5a, excluding two nucleotides from both ends (Figure 2A). We found that E5a-Δ4 and E5a-Δ5 decreased the $AChE_T$ isoform, indicating presence of splicing regulatory *cis*-elements in these blocks.

To further dissect *cis*-elements, we sequentially deleted eight 25-bp blocks in E5a-Δ4 and E5a-Δ5 (Figure 2B). We found that blocks E5a-Δ4d, E5a-Δ5b and E5a-Δ5c potentially harbor splicing regulatory *cis*-elements. A previously identified branch point sequence (BPS) in rat *Ache* (14) is mapped to E5a-Δ5b in human *ACHE*. The putative BPSs in E5a-Δ5b in human *ACHE* were at 304 to 317 nucleotides upstream to the distal 3′ ss (green letters in Supplementary Figure S5A). We serially substituted non-A nucleotides for A nucleotides in the putative BPSs (Supplementary Figure S5B). Among the six A nucleotides, substitution of the central four A nucleotides attenuated the usage of the distal 3′ ss, yielding a less amount of the $AChE_T$ isoform. Substitution of all six A nucleotides completely abolished the usage of the distal 3′ ss. A putative polypyrimidine tract spans blocks E5a-Δ5c and E5a-Δ5d (blue letters in Supplementary Figure S5A). Polypyrimidines in E5a-Δ5c are likely to be more essential than those in E5a-Δ5d, because E5a-Δ5c suppressed the usage of the distal 3′ ss more than E5a-Δ5d (Figure 2B). As there was no known splicing regulatory *cis*-element(s) in E5a-Δ4d, we next searched for *trans*-factors that bind to E5a-Δ4d and regulate alternative 3′ ss selection.

HnRNP H binds to the *cis*-element in E5a-Δ4d

Accumulating knowledge discloses that a vast majority of splicing silencers and enhancers are bound to and regulated by their cognate regulatory proteins (1). To determine *trans*-acting factor(s) that interact with E5a-Δ4d, we first searched for putative binding motifs of RNA-binding proteins using the human splicing factor database, SpliceAid 2 (40) (Supplementary Figure S6A). We introduced artificial mutations into E5a-Δ4d so that SpliceAid 2 predicted no RNA-binding proteins (Supplementary Figure S6B). We thus synthesized biotinylated wild-type (Wt-E5a) and mutant (Mut-E5a) RNA probes (Figure 2C), and performed an RNA affinity purification assay using nuclear extracts of SH-SY5Y cells. Coomassie blue staining of the RNA affinity purified proteins detected a distinct band at ∼55 kDa with Wt-E5a but not with Mut-E5a (Figure 2D). Using mass spectrometry, we found that the excised band was hnRNP H. We confirmed by immunoblotting that the bound proteins were hnRNP H and its paralog hnRNP F, although the amount of hnRNP F was much lower than that of hnRNP H (Figure 2E). As predicted by SpliceAid 2, we also observed weak binding of hnRNP A1 (Supplementary Figure S6A and S6C) to the Wt-E5a probe by immunoblotting, although we did not observe any distinct band for hnRNP A1 in the Coomassie blue stained gel (Figure 2D).

HnRNP H is a critical regulator for the selection of the distal 3′ ss

Having identified the candidate *trans*-acting factors, we next examined the effect of hnRNP H and F on alternative usage of the proximal and distal 3′ ss's by siRNA-mediated downregulation of the individual factors. We first confirmed by immunoblotting that siRNAs efficiently downregulate hnRNP H and F in SH-SY5Y cells (Figure 3A). Individual downregulation of hnRNP H slightly decreased the selection of distal 3′ ss, whereas downregulation of hnRNP F had no effect (Figure 3B). However, downregulation of both hnRNP H and F significantly reduced the selection of the distal 3′ ss, suggesting that hnRNP H and F are able to compensate for the lack of the counterpart. We also confirmed that overexpression of siRNA-resistant hnRNP H (si-res-hnRNP H) rescued the effect of the downregulation of hnRNP H/F (Figure 3C). Since hnRNP A1 showed a weak binding affinity for the Wt-E5a probe, we examined whether hnRNP A/B family of proteins have any effect on *ACHE*

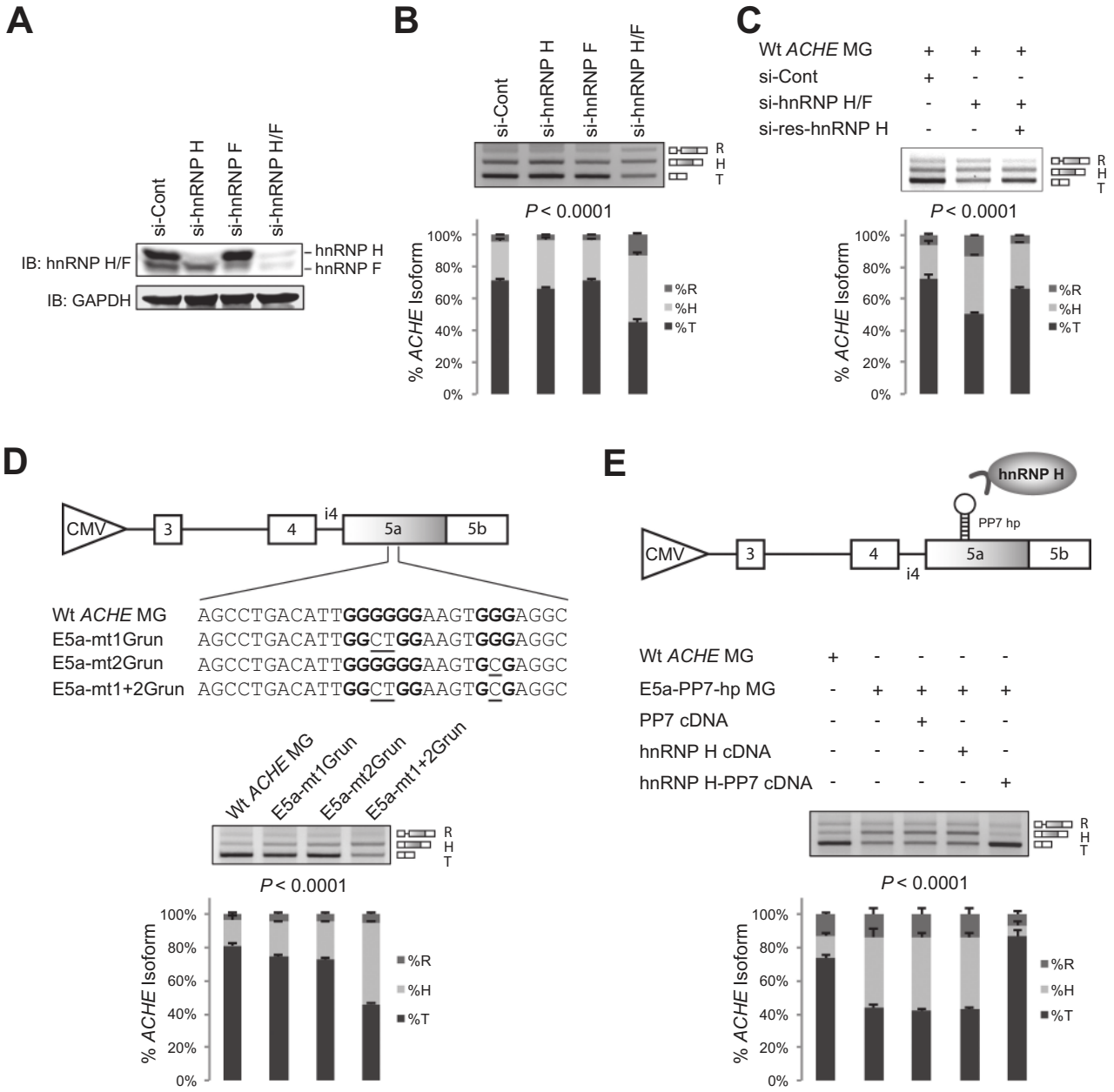

Figure 3. HnRNP H is a critical regulator of *ACHE* alternative splicing. (**A**) Immunoblotting (IB) with indicated antibodies of SH-SY5Y cell lysate after knockdown with siRNAs against control (si-Cont), *HNRNPH* (si-hnRNP H), *HNRNPF* (si-hnRNP F) and both *HNRNPH* and *HNRNPF* (si-hnRNP H/F). (**B**) RT-PCR of endogenous *ACHE* in SH-SY5Y cells treated with indicated siRNAs. (**C**) RT-PCR of *ACHE* minigene (MG) transfected in SH-SY5Y cells treated with si-hnRNP H/F with or without si-resistant hnRNP H cDNA. (**D**) Schematic of the *ACHE* minigenes (MG) carrying wild-type or mutant G-runs in exon 5a. G-runs are shown in bold and the introduced mutations are underlined. RT-PCR of wild-type and mutant constructs transfected in SH-SY5Y cell are shown. (**E**) Schematic of the *ACHE* minigene (MG) carrying the PP7 hairpin-loop substituting for two *cis*-acting G-runs in exon 5a (E5a-PP7-hp MG). HnRNP H is fused to the PP7 coat protein (inverted U shaped) to directly tether hnRNP H to the PP7 hairpin-loop. RT-PCR of minigenes cotransfected with the effector cDNAs in SH-SY5Y cells are shown. (**B**, **C**, **D** and **E**) Ratios of splicing isoforms of *ACHE* are shown in the stacked column graphs. Mean and SD are indicated ($n = 3$). *P*-values by two-way ANOVA are indicated above each graph. *P*-values by Tukey's multiple comparison test are indicated in Supplementary Table 2.

alternative splicing. Downregulation of hnRNP A1 had no effect on splicing of human *ACHE*, whereas knockdown of A2/B1 marginally shifted splicing from $AChE_T$ to $AChE_H$ and $AChE_R$ isoforms (Supplementary Figure S6D).

Specific G-runs in exon 5a coordinately regulate the selection of the distal 3′ ss

It is established that both hnRNP H and F bind to G-runs to regulate alternative splicing of numerous genes (20,21). There are two G-runs in E5a-Δ4d block (Figure 3D). To examine which G-run is crucial for splicing regulation, we

mutated either or both of the G-runs in the minigene construct. RT-PCR analysis revealed that disruption of a single G-run marginally affected splicing, whereas disruption of both G-runs resulted in a splicing shift towards the $AChE_H$ isoform from the $AChE_T$ isoform, indicating that at least one of these G-runs is required for the selection of the distal 3′ ss (Figure 3D).

Having identified the critical G-runs and their cognate binding partners, we next confirmed that hnRNP H exerts its effect by specifically binding to these motifs, not elsewhere. We introduced the bacteriophage PP7 coat protein-binding hairpin-loop in place of two G-runs in E5a-Δ4d. We also made a cDNA fusion construct encoding hnRNP H and PP7 coat protein, to artificially tether hnRNP H to the PP7 hairpin-loop. As expected, tethering of hnRNP H efficiently induced the selection of the distal 3′ ss (Figure 3E). Similar results were obtained by tethering of hnRNP F (Supplementary Figure S7C), indicating that both hnRNP H and F are able to upregulate the selection of the distal 3′ ss, yielding the $AChE_T$ isoform.

HnRNP H negatively regulates the usage of a cryptic PAS in exon 5a

Since AS and APA are closely-related mechanisms to regulate expressions of mRNA isoforms, we analyzed the usage of an alternative PAS in the human *ACHE* gene. We noticed a truncated *ACHE* transcript in most annotation databases of the human genome (Supplementary Figure S1), suggesting the presence of a cryptic PAS with a weak polyadenylation signal sequence, UAUAAA (41), in exon 5a (Figure 4A,B). The cleavage site of the cryptic PAS is located immediately upstream to the hnRNP H-binding site in exon 5a (Figure 5A). We first confirmed by 3′ RACE that SH-SY5Y cells use the cryptic PAS in exon 5a (pA-1) and the canonical PAS at the end of exon 5b (pA-2) (Figure 4B). Sequencing of the 3′ RACE products revealed that both the cryptic and canonical PASs are indeed used (Figure 4C).

We next questioned whether hnRNP H is involved in the selection of the cryptic PAS of *ACHE* pre-mRNA. The 3′ RACE analysis of endogenous *ACHE* in hnRNP H/F-knocked down SH-SY5Y cells revealed that downregulation of hnRNP H upregulated the selection of the cryptic PAS (higher pA-1/pA-2 ratio) (Figure 4D). This effect was rescued by overexpression of si-resistant hnRNP H. To dissect *cis*-acting elements that confer alternative PAS selection and to perform 3′ RACE specific for the minigene, we introduced artificial mutations at the 3′ end of priming sites of the nested forward primers and constructed the primer mutated (pm) *ACHE* minigene (Supplementary Figure S8). We confirmed that the pm-Wt *ACHE* minigene showed similar splicing pattern as the Wt *ACHE* minigene (Supplementary Figure S8). Similar to endogenous *ACHE*, knockdown of hnRNP H/F resulted in significantly increased selection of the cryptic PAS in the pm-Wt *ACHE* minigene (Figure 4E). We also confirmed that overexpression of si-res-hnRNP H rescued the effects of siRNA. These results suggest that hnRNP H suppresses the selection of the cryptic PAS and promotes the selection of the distal 3′ ss.

HnRNP H competes with the 3′ processing factor CstF64 to regulate alternative PAS recognition

We next analyzed the molecular mechanism of hnRNP H-mediated regulation of APA and investigated the relationship between APA and AS. CstF64 subunit, which is an essential 3′ processing factor, binds to GU/U-rich regions located within ∼40 nucleotides downstream of the cleavage site (2). Several UG-rich elements are present immediately downstream of the cleavage site, and are overlapping with the two essential G-runs in exon 5a, suggesting that hnRNP H and CstF64 may compete each other for RNA-binding (Figure 5A). We individually depleted hnRNP H/F and CstF64 from HeLa nuclear extracts (Figure 5B), and performed an RNA affinity purification assay using a biotinylated RNA probe carrying the cryptic PAS and its flanking regions (Figure 5A). Depletion of CstF64 resulted in increased binding of hnRNP H to the RNA probe (lane 3 in Figure 5C), whereas depletion of hnRNP H/F resulted in increased binding of CstF64 to the RNA probe (lane 2 in Figure 5C).

To further examine the molecular mechanism of coupled regulation of AS and APA, we introduced mutations to disrupt the cryptic PAS (UAUAAA>UAUUGA) in the pm-*ACHE* minigene, which resulted in exclusive selection of the canonical PAS (pA-2) (Figure 5D). We then converted the weak cryptic PAS to an optimal one (UAUAAA>AAUAAA), which resulted in efficient selection of pA-1. We introduced three G > T mutations in exon 5a to disrupt binding of hnRNP H/F, and simultaneously generate *de novo* binding motifs for CstF64. Disruption of the G-runs also resulted in increased usage of the cryptic PAS (Figure 5D). We next asked whether activation of the cryptic PAS could affect the expression of alternative *ACHE* isoforms. As expected, RT-PCR of the alternative *ACHE* isoforms revealed that the selection of the cryptic PAS was accompanied by the expression of $AChE_H$ isoform arising from these constructs (Figure 5D).

Expression levels of HnRNP H determine the abundance of $AChE_T$ in SH-SY5Y, Caco-2 and TF-1 cells

Variable expression levels of the alternative AChE isoforms were previously observed in certain cell lines (8). RT-PCR analysis showed that the alternative exon 5a is highly and moderately included in Caco-2 and TF-1 cells, respectively, compared to SH-SY5Y cells (Supplementary Figure S9A). In accordance with RT-PCR, 3′ RACE revealed that the selection of the cryptic PAS was ∼4-fold and ∼2.5-fold higher in Caco-2 and TF-1 cells, respectively, compared to SH-SY5Y cells (Supplementary Figure S9B). Further, in accordance with RT-PCR and 3′ RACE, immunoblotting revealed that the expression levels of hnRNP H were in descending order of SH-SY5Y, TF-1 and Caco-2 cells (Supplementary Figure S9C). In contrast, the expression level of CstF64 in Caco2 cells was higher than those in SH-SY5Y and TF-1 cells (Supplementary Figure S9C). Thus, expression levels of hnRNP H and CstF64 are reciprocally regulated in these cells, and the balance between hnRNP H and CstF64 determines the AChE isoforms and the usage of alternative PASs.

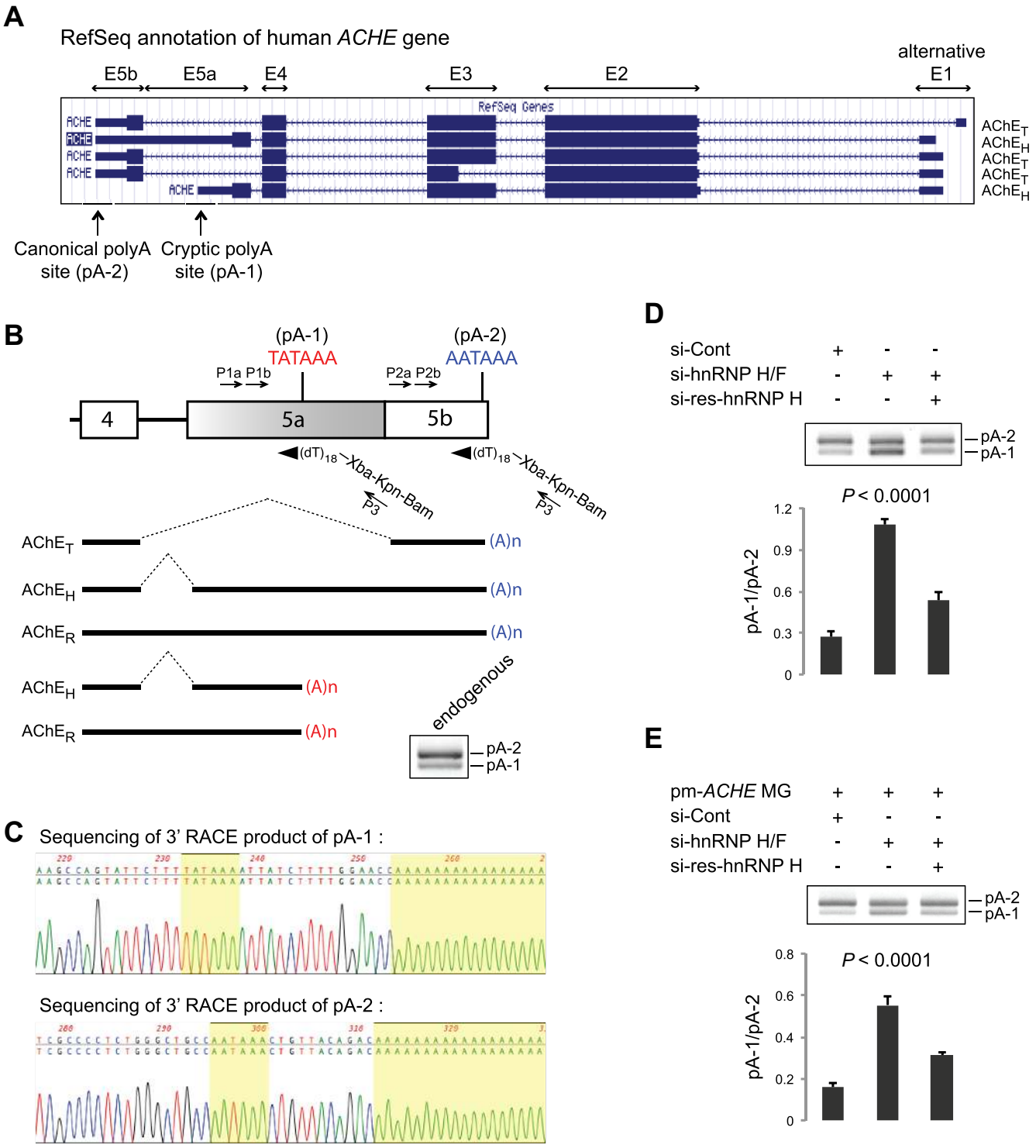

Figure 4. HnRNP H negatively regulates the selection of a cryptic PAS in exon 5a, which generates a short mRNA species of *ACHE*. (**A**) RefSeq annotation of human *ACHE* showing the presence of a short mRNA transcript of human *ACHE*. Arrows point to the canonical (pA-2) and cryptic (pA-1) PASs. Human *ACHE* is encoded on the opposite strand. (**B**) Schematic of two alternative polyA signals and possible *ACHE* isoforms. For 3′ RACE, cDNA is synthesized with a $(dT)_{18}$-primer carrying three restriction sites. Polyadenylated 3′ ends of endogenous *ACHE* in SH-SY5Y cells are amplified by RT-PCR with a mixture of P1a, P2a and P3 primers, followed by nested RT-PCR with a mixture of P1b, P2b and P3 primers, and run on a gel. (**C**) Sequencing results of the 3′ RACE products obtained in (**B**). PolyA signals and polyA tails are highlighted. (**D**) PASs of endogenous *ACHE* (**E**) or transfected *ACHE* minigene in SH-SY5Y cells are analyzed by 3′ RACE after knocking down hnRNP H/F with or without si-resistant hnRNP H. Mean and SD are indicated ($n = 3$). *P*-values by one-way ANOVA are indicated above each graph. *P*-values by Tukey's multiple comparison test are indicated in Supplementary Table 2.

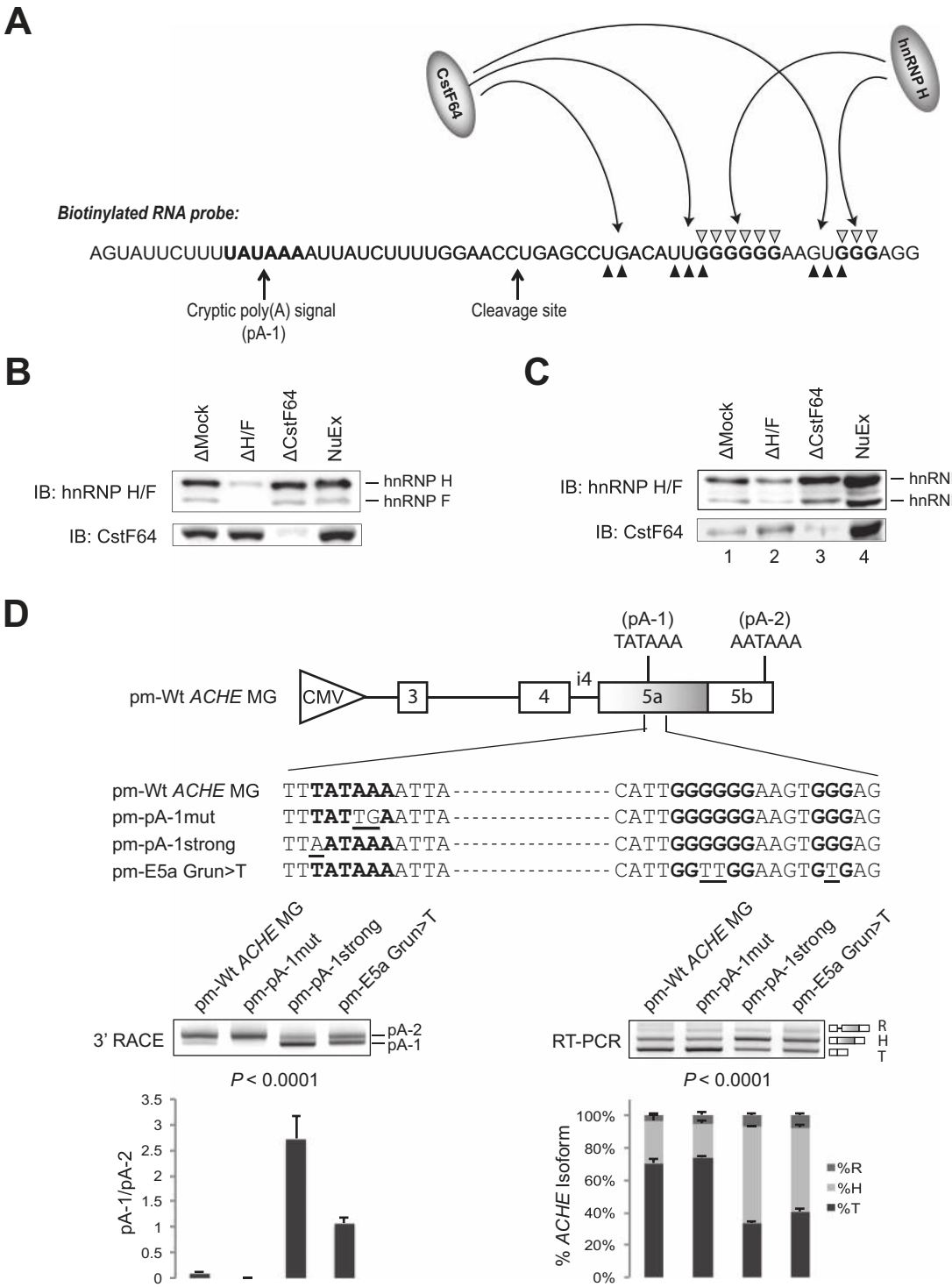

Figure 5. HnRNP H competes with a polyA factor, CstF64, to regulate alternative splicing and alternative PAS recognition. (**A**) Sequence of the wild-type biotinylated RNA probe containing the cryptic PAS (pA-1) and putative binding sites for hnRNP H (shaded arrowheads) and CstF64 (closed arrowheads). (**B**) IB of HeLa nuclear extracts depleted for control (ΔMock), hnRNP H/F (ΔH/F) and CstF64 (ΔCstF64). (**C**) IB of RNA affinity-purified HeLa nuclear extracts depleted for the indicated proteins using the RNA probe shown in (**A**). (**D**) Schematic of human *ACHE* minigenes with artificial mutations at the primer-binding sites (Supplementary Figure S8) to specifically recognize minigene transcripts (pm-Wt *ACHE* MG). Cryptic polyA signal (pA-1) is either mutated (pm-PA-1mut) or optimized (pm-pA-1strong). Alternatively, two *cis*-acting G-runs are mutated (pm-E5a Grun>T). Representative 3′ RACE and RT-PCR of these constructs transfected in SH-SY5Y cells are shown. Mean and SD are indicated ($n = 3$). *P*-values by one-way ANOVA or two-way ANOVA are indicated above each graph. *P*-values by Tukey's multiple comparison test are indicated in Supplementary Table 2.

HnRNP H suppresses APA and activates the distal 3′ ss in many other genes

We have shown that expression of the AChE isoforms is controlled by hnRNP H-mediated antagonizing regulation of alternative selection of the distal 3′ ss and the cryptic PAS. In order to examine whether this is generally observed in human, we analyzed RNA-seq of *HNRNPH*-knocked down HEK 293T cells (GSE16642) and CLIP-seq of hnRNP H in HEK 293T cells (GSE23694) in the GEO database (32). Clustering of CLIP-tags of hnRNP H (GSE23694) upstream to the hnRNP H-activated APA sites was previously reported (32). We detected 43 152 transcripts with different APA sites. Out of the 43 152 APA sites, the splicing analysis tool for RNA-seq, MISO, revealed that 635 APA sites are located between a constitutive 5′ ss and an alternative distal 3′ ss, and are in proximity to an alternative proximal 3′ ss, as we observed in the human *ACHE* gene. To evaluate the effect of hnRNP H on the selection of an APA site and an alternative 3′ ss, we divided the APA sites into five categories from the most activated APA sites to the most downregulated APA sites by hnRNP H. Similar to the human *ACHE* gene, APA sites that were suppressed by hnRNP H were associated with the selection of the distal alternative 3′ ss's (Figure 6).

HnRNP H exerts no overt effect on functions mediated by *ACHE* isoforms

We next examined the effect of hnRNP H on alternative 5′ exons and on previously reported functions of *ACHE* isoforms. First, according to the EST database, at least four alternative 5′ exons exist in human *ACHE* (E1a, E1b, E1c and E1d), and that E1b is preferentially used as the default 5′ exon (42). Unlike alternative regulations of the 3′ ss and polyadenylation sites by hnRNP H, knocking down of hnRNP H had no effect on usage of the alternative 5′ exons in SH-SY5Y cells (Supplementary Figure S10). Second, Perry *et al*. showed that ASP_{67} (C-terminal peptide of $AChE_T$ or AChE-S) interacts with a transcriptional co-repressor CtBP and co-localizes in the nucleus and modify the function of Ikaros, causing T lymphopenia (43). We found that nuclear localization of ASP_{67} was not affected by knocking down of hnRNP H in SH-SY5Y cells (Supplementary Figure S11). Third, N-terminally extended $AChE_T$ isoform (N-AChE-S or N-$AChE_T$) induces caspase-mediated cell death in mouse primary cortical cells (44). Downregulation of hnRNP H/F, however, did not affect the survival of SH-SY5Y cells (Supplementary Figure S12). Fourth, cellular differentiation modifies alternative splicing of many genes and raises a question whether the splicing pattern of human *ACHE* gene is also changed with differentiation. We found that neuronal differentiation of SH-SY5Y cells had a marginal effect on the relative expression of alternatively spliced *ACHE* isoforms (Supplementary Figure S13).

DISCUSSION

We have analyzed the molecular mechanisms underlying generation of human *ACHE* isoforms, and have shown that alternative splicing of *ACHE* is coupled to selection of an APA site, which is coordinately regulated by hnRNP H and its antagonizing CstF64. In human *ACHE*, hnRNP H activates the selection of the distal 3′ ss, which produces the muscle- and brain-specific $AChE_T$ isoform (Figure 7). On the contrary, lack of hnRNP H allows CstF64 to bind downstream to the cryptic PAS (pA-1), which generates a truncated transcript lacking the distal 3′ ss. Two alternative choices for this short transcript are either to select the proximal 3′ ss ($AChE_H$) or to retain intron 4 ($AChE_R$) (Figure 7). Similar effects of hnRNP H on both activation of the distal 3′ ss and suppression of APA are observed in global analysis of CLIP-seq and RNA-seq (Figure 6).

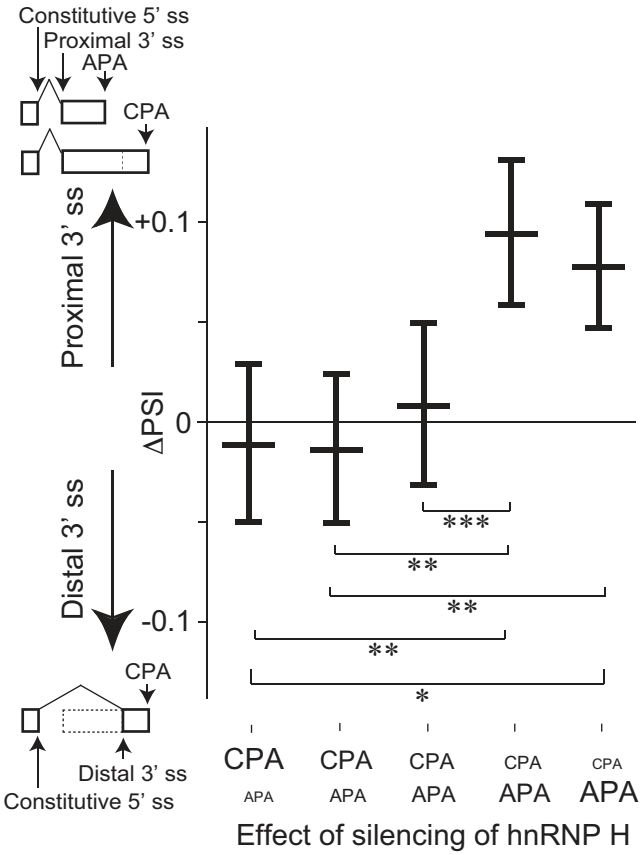

Figure 6. Suppression and activation of APA by silencing hnRNP H are coupled to the selection of the distal and proximal 3′ ss's, respectively. An APA is located between the constitutive 5′ ss and the distal alternative 3′ ss in 635 genes in the human genome. RNA-seq analysis reveals that silencing of hnRNP H activates constitutive polyadenylation (CPA) sites in some of the 635 genes, whereas it activates APA sites in some others of the 635 genes. The 635 genes are evenly divided into five groups according to the effect of hnRNP H silencing on APA activation. For each group, RNA-seq coverage between the proximal and distal 3′ ss's are counted. The difference in coverage after knocking down hnRNP H is indicated by the mean and 95% confidence interval of ΔPSI (percent-spliced-in) by MISO software. A positive ΔPSI value indicates that RNA-seq coverage between the proximal and distal 3′ ss's is increased by hnRNP H silencing. Two of the five groups of the 635 genes show positive ΔPSI values. This indicates that in genes, in which APA is activated by hnRNP H silencing, the proximal 3′ ss is selected by hnRNP H silencing. In other words, in genes, in which APA is suppressed by hnRNP H, the distal 3′ ss is activated by hnRNP H, as we observed with *ACHE*. $P < 0.001$ by Kruskal–Wallis test. $^*P < 0.05$, $^{**}P < 0.01$ and $^{***}P < 0.001$ by Steel–Dwass post-hoc test.

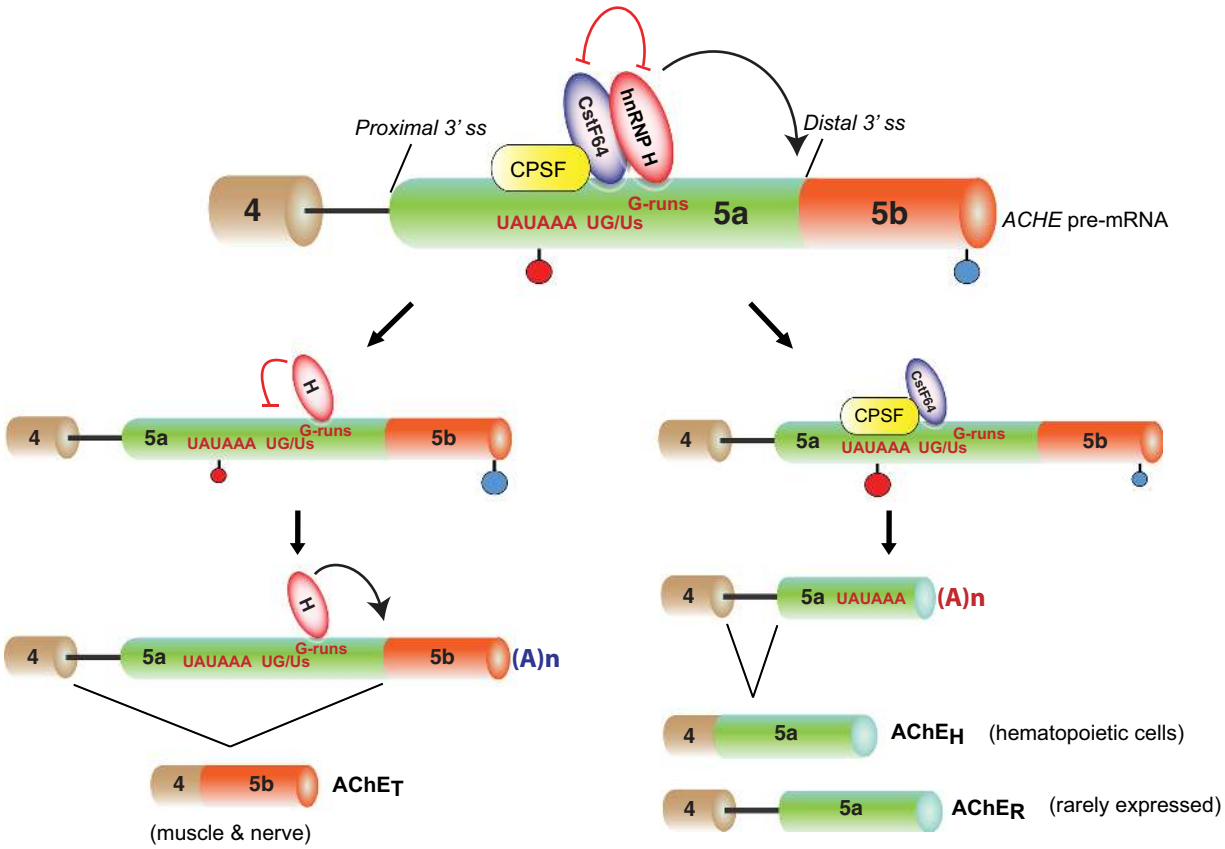

Figure 7. Schematic showing competition between hnRNP H-mediated activation of the distal 3′ ss generating AChE$_T$ and CstF64-mediated activation of the cryptic PAS (UAUAAA) generating AChE$_H$ and AChE$_R$. Exons and introns are indicated by cylinders and solid lines, respectively. The cryptic (pA-1) and canonical (pA-2) PASs are marked by red and blue closed circles, respectively. HnRNP H-binding G-runs and CstF64-binding UG/Us are overlapping, and hnRNP H and CstF64 compete for binding to exon 5a. In cells expressing a high amount of hnRNP H, hnRNP H binds to exon 5a and activates the distal 3′ ss to generate AChE$_T$. In contrast, in cells expressing a low amount of hnRNP H, CstF64 wins the binding and activates pA-1 to generate AChE$_H$ and AChE$_R$.

Guerra *et al*. previously identified that the branch point for the distal 3′ ss is located 278 nucleotides upstream to the distal 3′ ss in rat *Ache* (14). We have shown that human *ACHE* carries six redundant branch point A nucleotides at 304–317 nucleotides upstream to the distal 3′ ss (Supplementary Figure S5). Redundancy in the branch point A nucleotides has been repeatedly reported in other genes (45–47). We previously reported that the average distance between the branch point and the 3′ ss is 21 to 34 nucleotides in human genes (46). The branch points of rat *Ache* and human *ACHE* are thus unusually far from the 3′ ss. Interestingly, previous reports show that muscle-specific exons of *Tpm1* encoding α-tropomyosin (48), *Tpm2* encoding β-tropomyosin (49) and *Actn1* encoding α-actinin (50) have branch points unusually far from the 3′ ss. A branch point unusually far from the 3′ ss may be exploited to generate muscle-specific isoforms in some genes, but the underlying mechanisms remain to be dissected. HnRNP H-binding site that we analyzed in this communication is ∼40 nucleotides upstream of the branch point in human *ACHE*, and hnRNP H is unlikely to be involved in recognition of the branch point. Sequence alignments of exons 4 to 5b of human *ACHE* with those of mouse and rat *Ache* show that this region is poorly conserved between these species (Supplementary Figure S2). However, conservation is observed in E5a-Δ4c and E5a-Δ4d harboring the cryptic PAS (pA-1) and the splicing regulatory G-runs (Supplementary Figure S2B), as well as in E5a-Δ5b and E5a-Δ5c carrying the putative branch points and the polypyrimidine tract (Supplementary Figure S2C). Human *ACHE*, mouse *Ache* and rat *Ache* are thus likely to use similar coupled regulation of alternative splicing and alternative polyadenylation to generate the AChE isoforms.

There are two G-runs in the identified *cis*-regulatory region, and disruption of a single G-run has a marginal effect on the selection of the distal 3′ ss (Figure 3D). In contrast, we previously reported that disruption of a single G-run in intron 3 of *CHRNA1* compromises binding of hnRNP H, and causes aberrant inclusion of the downstream exon P3A in congenital myasthenic syndrome (CMS) (25,51). Similarly, but oppositely, a GGAGG-to-GGGGG mutation in exon 16 of *COLQ de novo* gains binding of hnRNP H, and causes skipping of exon 16 in CMS (24). Synergistic splicing regulation by multiple G-runs has been reported in *THPO* encoding thrombopoietin (52), *CBS* encoding cystathionine β-synthase (53) and *HBA1* encoding α-globin (54). Multiple binding of hnRNP H to G-runs is likely to ensure

proper recognition of its cognate sequence, and disruption of a single G-run is tolerable in some but not all genes.

In human *ACHE*, hnRNP H plays dual regulatory roles: enhancement of the selection of the distal 3′ ss and inhibition of the selection of the cryptic PAS. In contrast to *ACHE*, binding of hnRNP H to G-rich elements (GRE) downstream to a PAS promotes recruitment of CstF64 for subsequent 3′ end-processing in pre-mRNAs of viral genes for SVL40, AAV, IVA2 and AdL3 (29,55), as well as mammalian genes for immunoglobulin M (IgM) (29,55) and p53 (28). Similarly, binding of hnRNP H either upstream or downstream to a PAS promotes recruitment of poly(A) polymerase in β-globin pre-mRNA (56). Interestingly, binding of hnRNP F, but not hnRNP H, to GRE elements downstream to a PAS of the IgM pre-mRNA in B cells (31), as well as of SVL40 pre-mRNA (30), suppresses binding of CstF64. In contrast to these previous reports demonstrating that hnRNP H enhances and hnRNP F suppresses 3′ end processing, binding of both hnRNP H and F downstream to the cryptic PAS displaces binding of CstF64 and suppresses the relevant PAS in human *ACHE* (Figure 5A–C).

As summarized in Supplementary Table 3, hnRNP H and F exert similar or dissimilar effects on alternative RNA metabolisms. Similar effects, as we observed with *ACHE*, are reported in three genes. First, hnRNP H and F silence *FGFR2* exon IIIc by forming a complex with Fox2 (18). HnRNP H competes with SRSF1 for binding to exon IIIc, but the effect of hnRNP F on SRSF1 is not analyzed (18). Second, hnRNP H and hnRNP F recruit U1snRNP and activate the upstream 5′ splice site of *PLP1* exon 3 *in vitro* (57). *In vivo*, however, tethering of hnRNP H, but not of hnRNP F, activates the upstream 5′ splice site of *PLP1* exon 3 (57). Third, hnRNP H and F are both components of a splicing enhancer complex that activates *Src* exon N1 (22). Immunodepletion of hnRNP H inactivates splicing of *Src* exon N1 *in vitro*, which cannot be restored by recombinant hnRNP F (22). In our study, the expression levels of hnRNP H determine the abundance of $AChE_T$ isoform in three cell lines, whereas the expression levels of hnRNP F are much lower than those of hnRNP H in these cell lines (Supplementary Figure S9). These findings suggest that hnRNP H plays a major regulatory role in splicing regulation in the human *ACHE* gene and hnRNP F has partial additive effect on this regulation. Downregulation of hnRNP H alone partially but significantly decreases selection of the distal 3′ ss ($AChE_T$ isoform), with concomitant increase in the expression of $AChE_H$ isoform (Figure 3B). However, more prominent effect is observed when both hnRNP H and F are knocked-down together. This is likely because hnRNP F compensates for the lack of hnRNP H. Similar effects of hnRNP H on coupled regulation of AS and APA are observed in other genes in bioinformatic analysis (Figure 6). If RNA-seq after knocking down both hnRNP H and F were available, we might have been able to observe more distinct effects.

iCLIP and RNA-seq analyses of CstF64 demonstrated that CstF64 binds to thousands of cryptic intronic PASs and activate these APA sites (58). Interestingly, these APA sites are suppressed, in part, by U1 small nuclear ribonucleoproteins (U1 snRNPs), which is a fundamental 5′ ss recognition factor in pre-mRNA splicing (2). Furthermore, two essential factors for processing the 3′ end of mRNA, cleavage and polyadenylation specificity factor and Symplekin regulate AS of internal exons (59). Dissection of regulatory mechanisms of human *ACHE* isoforms (Figures 1-5), as well as global analysis of the effect of hnRNP H on AS and APA (Figure 6), reveal that hnRNP H is another essential factor that confers coupled regulation of AS and APA.

SUPPLEMENTARY DATA

Supplementary Data are available at NAR Online.

ACKNOWLEDGEMENTS

GFP-tagged ASP_{67} (GFP-ASP_{67}) and GFP-tagged ARP_{51} (GFP-ARP_{51}) were kindly provided by Dr Hermona Soreq at Hebrew University. The authors thank Kentaro Taki (Nagoya University Graduate School of Medicine) for his technical assistance on the mass spectrometry analysis.

FUNDING

Ministry of Education, Culture, Sports, Science and Technology (MEXT); Ministry of Health, Labour and Welfare (MHLW); Japan Agency for Medical Research and Development (AMED) of Japan. Funding for open access charge: MEXT of Japan.
Conflict of interest statement. None declared.

REFERENCES

1. Black,D.L. (2003) Mechanisms of alternative pre-messenger RNA splicing. *Annu. Rev. Biochem.*, **72**, 291–336.
2. Shi,Y. and Manley,J.L. (2015) The end of the message: multiple protein-RNA interactions define the mRNA polyadenylation site. *Genes Dev.*, **29**, 889–897.
3. Wang,E.T., Sandberg,R., Luo,S., Khrebtukova,I., Zhang,L., Mayr,C., Kingsmore,S.F., Schroth,G.P. and Burge,C.B. (2008) Alternative isoform regulation in human tissue transcriptomes. *Nature*, **456**, 470–476.
4. Keren,H., Lev-Maor,G. and Ast,G. (2010) Alternative splicing and evolution: diversification, exon definition and function. *Nat. Rev. Genet.*, **11**, 345–355.
5. Hoque,M., Ji,Z., Zheng,D., Luo,W., Li,W., You,B., Park,J.Y., Yehia,G. and Tian,B. (2013) Analysis of alternative cleavage and polyadenylation by 3′ region extraction and deep sequencing. *Nat. Methods*, **10**, 133–139.
6. Soreq,H. and Seidman,S. (2001) Acetylcholinesterase – new roles for an old actor. *Nat. Rev. Neurosci.*, **2**, 294–302.
7. Li,Y., Camp,S. and Taylor,P. (1993) Tissue-specific expression and alternative mRNA processing of the mammalian acetylcholinesterase gene. *J. Biol. Chem.*, **268**, 5790–5797.
8. Bi,C.W., Luk,W.K., Campanari,M.L., Liu,Y.H., Xu,L., Lau,K.M., Xu,M.L., Choi,R.C., Saez-Valero,J. and Tsim,K.W. (2014) Quantification of the transcripts encoding different forms of AChE in various cell types: real-time PCR coupled with standards in revealing the copy number. *J. Mol. Neurosci.*, **53**, 461–468.
9. Luk,W.K., Chen,V.P., Choi,R.C. and Tsim,K.W. (2012) N-linked glycosylation of dimeric acetylcholinesterase in erythrocytes is essential for enzyme maturation and membrane targeting. *FEBS J.*, **279**, 3229–3239.
10. Massoulie,J., Anselmet,A., Bon,S., Krejci,E., Legay,C., Morel,N. and Simon,S. (1998) Acetylcholinesterase: C-terminal domains, molecular forms and functional localization. *J. Physiol. Paris*, **92**, 183–190.
11. Massoulie,J. (2002) The origin of the molecular diversity and functional anchoring of cholinesterases. *Neurosignals*, **11**, 130–143.

12. Meshorer,E. and Soreq,H. (2006) Virtues and woes of AChE alternative splicing in stress-related neuropathologies. *Trends Neurosci.*, **29**, 216–224.
13. Li,Y., Camp,S., Rachinsky,T.L., Getman,D. and Taylor,P. (1991) Gene structure of mammalian acetylcholinesterase. Alternative exons dictate tissue-specific expression. *J. Biol. Chem.*, **266**, 23083–23090.
14. Guerra,M., Dobbertin,A. and Legay,C. (2008) Identification of cis-acting elements involved in acetylcholinesterase RNA alternative splicing. *Mol. Cell Neurosci.*, **38**, 1–14.
15. Meshorer,E., Bryk,B., Toiber,D., Cohen,J., Podoly,E., Dori,A. and Soreq,H. (2005) SC35 promotes sustainable stress-induced alternative splicing of neuronal acetylcholinesterase mRNA. *Mol. Psychiatry*, **10**, 985–997.
16. Deschenes-Furry,J., Belanger,G., Perrone-Bizzozero,N. and Jasmin,B.J. (2003) Post-transcriptional regulation of acetylcholinesterase mRNAs in nerve growth factor-treated PC12 cells by the RNA-binding protein HuD. *J. Biol. Chem.*, **278**, 5710–5717.
17. Deschenes-Furry,J., Belanger,G., Mwanjewe,J., Lunde,J.A., Parks,R.J., Perrone-Bizzozero,N. and Jasmin,B.J. (2005) The RNA-binding protein HuR binds to acetylcholinesterase transcripts and regulates their expression in differentiating skeletal muscle cells. *J. Biol. Chem.*, **280**, 25361–25368.
18. Mauger,D.M., Lin,C. and Garcia-Blanco,M.A. (2008) hnRNP H and hnRNP F complex with Fox2 to silence fibroblast growth factor receptor 2 exon IIIc. *Mol. Cell. Biol.*, **28**, 5403–5419.
19. Van Dusen,C.M., Yee,L., McNally,L.M. and McNally,M.T. (2010) A glycine-rich domain of hnRNP H/F promotes nucleocytoplasmic shuttling and nuclear import through an interaction with transportin 1. *Mol. Cell. Biol.*, **30**, 2552–2562.
20. Wang,E., Aslanzadeh,V., Papa,F., Zhu,H., de la Grange,P. and Cambi,F. (2012) Global profiling of alternative splicing events and gene expression regulated by hnRNPH/F. *PLoS One*, **7**, e51266.
21. Xiao,X., Wang,Z., Jang,M., Nutiu,R., Wang,E.T. and Burge,C.B. (2009) Splice site strength-dependent activity and genetic buffering by poly-G runs. *Nat. Struct. Mol. Biol.*, **16**, 1094–1100.
22. Chou,M.Y., Rooke,N., Turck,C.W. and Black,D.L. (1999) hnRNP H is a component of a splicing enhancer complex that activates a c-src alternative exon in neuronal cells. *Mol. Cell. Biol.*, **19**, 69–77.
23. Garneau,D., Revil,T., Fisette,J.F. and Chabot,B. (2005) Heterogeneous nuclear ribonucleoprotein F/H proteins modulate the alternative splicing of the apoptotic mediator Bcl-x. *J. Biol. Chem.*, **280**, 22641–22650.
24. Rahman,M.A., Azuma,Y., Nasrin,F., Takeda,J., Nazim,M., Bin Ahsan,K., Masuda,A., Engel,A.G. and Ohno,K. (2015) SRSF1 and hnRNP H antagonistically regulate splicing of COLQ exon 16 in a congenital myasthenic syndrome. *Sci. Rep.*, **5**, 13208.
25. Masuda,A., Shen,X.M., Ito,M., Matsuura,T., Engel,A.G. and Ohno,K. (2008) hnRNP H enhances skipping of a nonfunctional exon P3A in CHRNA1 and a mutation disrupting its binding causes congenital myasthenic syndrome. *Hum. Mol. Genet.*, **17**, 4022–4035.
26. Crawford,J.B. and Patton,J.G. (2006) Activation of alpha-tropomyosin exon 2 is regulated by the SR protein 9G8 and heterogeneous nuclear ribonucleoproteins H and F. *Mol. Cell. Biol.*, **26**, 8791–8802.
27. Coles,J.L., Hallegger,M. and Smith,C.W. (2009) A nonsense exon in the Tpm1 gene is silenced by hnRNP H and F. *RNA*, **15**, 33–43.
28. Decorsiere,A., Cayrel,A., Vagner,S. and Millevoi,S. (2011) Essential role for the interaction between hnRNP H/F and a G quadruplex in maintaining p53 pre-mRNA 3′-end processing and function during DNA damage. *Genes Dev.*, **25**, 220–225.
29. Chen,F. and Wilusz,J. (1998) Auxiliary downstream elements are required for efficient polyadenylation of mammalian pre-mRNAs. *Nucleic Acids Res.*, **26**, 2891–2898.
30. Alkan,S.A., Martincic,K. and Milcarek,C. (2006) The hnRNPs F and H2 bind to similar sequences to influence gene expression. *Biochem J.*, **393**, 361–371.
31. Veraldi,K.L., Arhin,G.K., Martincic,K., Chung-Ganster,L.H., Wilusz,J. and Milcarek,C. (2001) hnRNP F influences binding of a 64-kilodalton subunit of cleavage stimulation factor to mRNA precursors in mouse B cells. *Mol. Cell. Biol.*, **21**, 1228–1238.
32. Katz,Y., Wang,E.T., Airoldi,E.M. and Burge,C.B. (2010) Analysis and design of RNA sequencing experiments for identifying isoform regulation. *Nat. Methods*, **7**, 1009–1015.
33. Nasrin,F., Rahman,M.A., Masuda,A., Ohe,K., Takeda,J. and Ohno,K. (2014) HnRNP C, YB-1 and hnRNP L coordinately enhance skipping of human MUSK exon 10 to generate a Wnt-insensitive MuSK isoform. *Sci. Rep.*, **4**, 6841.
34. Masuda,A., Takeda,J., Okuno,T., Okamoto,T., Ohkawara,B., Ito,M., Ishigaki,S., Sobue,G. and Ohno,K. (2015) Position-specific binding of FUS to nascent RNA regulates mRNA length. *Genes Dev.*, **29**, 1045–1057.
35. Kim,D., Pertea,G., Trapnell,C., Pimentel,H., Kelley,R. and Salzberg,S.L. (2013) TopHat2: accurate alignment of transcriptomes in the presence of insertions, deletions and gene fusions. *Genome Biol.*, **14**, R36.
36. Li,H. and Durbin,R. (2009) Fast and accurate short read alignment with Burrows-Wheeler transform. *Bioinformatics*, **25**, 1754–1760.
37. Trapnell,C., Williams,B.A., Pertea,G., Mortazavi,A., Kwan,G., van Baren,M.J., Salzberg,S.L., Wold,B.J. and Pachter,L. (2010) Transcript assembly and quantification by RNA-Seq reveals unannotated transcripts and isoform switching during cell differentiation. *Nat. Biotechnol.*, **28**, 511–515.
38. Li,H., Handsaker,B., Wysoker,A., Fennell,T., Ruan,J., Homer,N., Marth,G., Abecasis,G. and Durbin,R. (2009) The Sequence Alignment/Map format and SAMtools. *Bioinformatics*, **25**, 2078–2079.
39. Quinlan,A.R. and Hall,I.M. (2010) BEDTools: a flexible suite of utilities for comparing genomic features. *Bioinformatics*, **26**, 841–842.
40. Piva,F., Giulietti,M., Burini,A.B. and Principato,G. (2012) SpliceAid 2: A database of human splicing factors expression data and RNA target motifs. *Hum. Mutat.*, **33**, 81–85.
41. Silver Key,S.C. and Pagano,J.S. (1997) A noncanonical poly(A) signal, UAUAAA, and flanking elements in Epstein-Barr virus DNA polymerase mRNA function in cleavage and polyadenylation assays. *Virology*, **234**, 147–159.
42. Meshorer,E., Toiber,D., Zurel,D., Sahly,I., Dori,A., Cagnano,E., Schreiber,L., Grisaru,D., Tronche,F. and Soreq,H. (2004) Combinatorial complexity of 5′ alternative acetylcholinesterase transcripts and protein products. *J. Biol. Chem.*, **279**, 29740–29751.
43. Perry,C., Pick,M., Podoly,E., Gilboa-Geffen,A., Zimmerman,G., Sklan,E.H., Ben-Shaul,Y., Diamant,S. and Soreq,H. (2007) Acetylcholinesterase/C terminal binding protein interactions modify Ikaros functions, causing T lymphopenia. *Leukemia*, **21**, 1472–1480.
44. Toiber,D., Berson,A., Greenberg,D., Melamed-Book,N., Diamant,S. and Soreq,H. (2008) N-acetylcholinesterase-induced apoptosis in Alzheimer's disease. *PLoS One*, **3**, e3108.
45. Ohno,K., Tsujino,A., Shen,X.M., Milone,M. and Engel,A.G. (2005) Spectrum of splicing errors caused by CHRNE mutations affecting introns and intron/exon boundaries. *J. Med. Genet.*, **42**, e53.
46. Gao,K., Masuda,A., Matsuura,T. and Ohno,K. (2008) Human branch point consensus sequence is yUnAy. *Nucleic Acids Res.*, **36**, 2257–2267.
47. Ruskin,B., Greene,J.M. and Green,M.R. (1985) Cryptic branch point activation allows accurate in vitro splicing of human beta-globin intron mutants. *Cell*, **41**, 833–844.
48. Smith,C.W. and Nadal-Ginard,B. (1989) Mutually exclusive splicing of alpha-tropomyosin exons enforced by an unusual lariat branch point location: Implications for constitutive splicing. *Cell*, **56**, 749–758.
49. Helfman,D.M. and Ricci,W.M. (1989) Branch point selection in alternative splicing of tropomyosin pre-mRNAs. *Nucleic Acids Res.*, **17**, 5633–5650.
50. Southby,J., Gooding,C. and Smith,C.W. (1999) Polypyrimidine tract binding protein functions as a repressor to regulate alternative splicing of alpha-actinin mutally exclusive exons. *Mol. Cell. Biol.*, **19**, 2699–2711.
51. Bian,Y., Masuda,A., Matsuura,T., Ito,M., Okushin,K., Engel,A.G. and Ohno,K. (2009) Tannic acid facilitates expression of the polypyrimidine tract binding protein and alleviates deleterious inclusion of CHRNA1 exon P3A due to an hnRNP H-disrupting mutation in congenital myasthenic syndrome. *Hum. Mol. Genet.*, **18**, 1229–1237.
52. Marcucci,R., Baralle,F.E. and Romano,M. (2007) Complex splicing control of the human Thrombopoietin gene by intronic G runs. *Nucleic Acids Res.*, **35**, 132–142.
53. Romano,M., Marcucci,R., Buratti,E., Ayala,Y.M., Sebastio,G. and Baralle,F.E. (2002) Regulation of 3′ splice site selection in the

844ins68 polymorphism of the cystathionine Beta -synthase gene. *J. Biol. Chem.*, **277**, 43821–43829.
54. McCullough,A.J. and Berget,S.M. (1997) G triplets located throughout a class of small vertebrate introns enforce intron borders and regulate splice site selection. *Mol. Cell. Biol.*, **17**, 4562–4571.
55. Bagga,P.S., Arhin,G.K. and Wilusz,J. (1998) DSEF-1 is a member of the hnRNP H family of RNA-binding proteins and stimulates pre-mRNA cleavage and polyadenylation in vitro. *Nucleic Acids Res.*, **26**, 5343–5350.
56. Millevoi,S., Decorsiere,A., Loulergue,C., Iacovoni,J., Bernat,S., Antoniou,M. and Vagner,S. (2009) A physical and functional link between splicing factors promotes pre-mRNA 3′ end processing. *Nucleic Acids Res.*, **37**, 4672–4683.
57. Wang,E. and Cambi,F. (2009) Heterogeneous nuclear ribonucleoproteins H and F regulate the proteolipid protein/DM20 ratio by recruiting U1 small nuclear ribonucleoprotein through a complex array of G runs. *J. Biol. Chem.*, **284**, 11194–11204.
58. Yao,C., Biesinger,J., Wan,J., Weng,L., Xing,Y., Xie,X. and Shi,Y. (2012) Transcriptome-wide analyses of CstF64-RNA interactions in global regulation of mRNA alternative polyadenylation. *Proc. Natl. Acad. Sci. U.S.A.*, **109**, 18773–18778.
59. Misra,A., Ou,J., Zhu,L.J. and Green,M.R. (2015) Global Promotion of Alternative Internal Exon Usage by mRNA 3′ End Formation Factors. *Mol. Cell*, **58**, 819–831.